

# 1 MAXIMIZATION OF MONOMERIC C5 SUGARS FROM WHEAT 2 BRAN BY USING MESOPOROUS ORDERED SILICA 3 CATALYSTS

4 Nuria Sánchez-Bastardo, Esther Alonso\*

5 \*Corresponding author: High Pressure Processes Group -Chemical Engineering and  
6 Environmental Technology Department, C/Dr. Mergelina s/n, University of Valladolid, 47011,  
7 Spain, +34 983 42 31 75, ealonso@iq.uva.es

8

## 9 Abstract

10 The hydrolysis process of real a fraction of arabinoxylans derived from wheat bran was studied  
11 using different mesoporous silica materials and the corresponding  $\text{RuCl}_3$  catalysts in water. The  
12 influence of type and catalyst loading, reaction time and different metal cations were discussed  
13 in terms of the hydrolysis yield of arabinose and xylose oligomers as well as the formation of  
14 furfural as degradation product. A high yield of arabinoxylans into the corresponding  
15 monomeric sugars (96 and 94% from arabino- and xylo-oligosaccharides, respectively) was  
16 obtained at relatively high temperatures (180 °C) and short reaction times (15 min) with a  
17 catalyst loading of 4.8 g of  $\text{RuCl}_3/\text{Al-MCM-48}$  per g of initial carbon in hemicelluloses.

18 **Keywords:** arabinoxylan hydrolysis, wheat bran, biomass, heterogeneous catalysis, ruthenium  
19 catalysts.

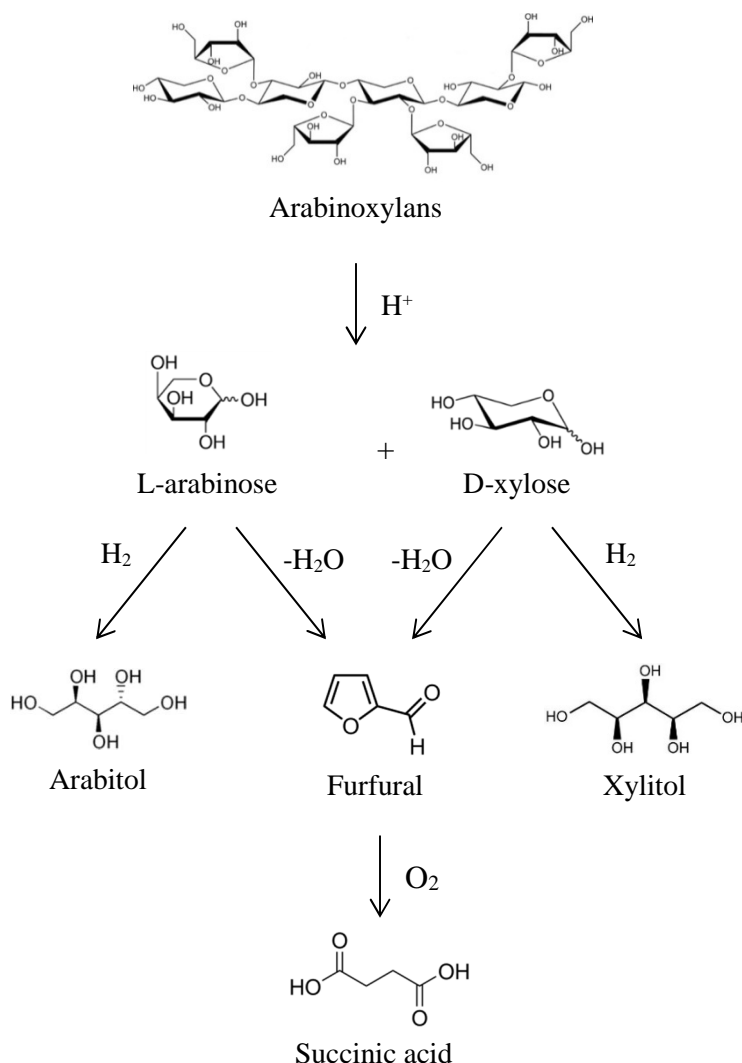
## 20 Highlights:

- 21 -  $\text{RuCl}_3/\text{Al-MCM-48}$  is an active catalyst for arabinoxylan hydrolysis.
- 22 -  $\text{RuCl}_3/\text{Al-MCM-48}$  accelerates conversion of arabinoxylans into arabinose and xylose.
- 23 -  $\text{RuCl}_3/\text{Al-MCM-48}$  catalysts inhibit further dehydration into furfural.
- 24 - Significant reduction in hydrolysis time from several hours to 15 min is achieved.
- 25 - A two-step process using  $\text{RuCl}_3/\text{Al-MCM-48}$  maximizes C5 sugars from wheat bran.

## 26 1. Introduction

27 The current depletion of fossil resources is forcing society to seek renewable alternatives for  
28 energy and chemicals production. Biomass is considered a sustainable and renewable feedstock  
29 to substitute fossil-based fuels (Negahdar et al., 2016; Oh et al., 2015; Putro et al., 2016;  
30 Singhvi et al., 2014). Biomass accrues in large amounts all over the world as forestry and  
31 agricultural waste. Moreover, around 95% of this biomass consists of lignocellulosic material  
32 not edible for humans. Thus, its application to biofuels or chemicals synthesis does not compete  
33 with food production (Negahdar et al., 2016; Sahu and Dhepe, 2012).

34 Agricultural residues like straw, corn stover or wheat bran appear as interesting feedstocks to  
35 obtain high added-value products (Apprich et al., 2014). Wheat bran is a by-product of the  
36 wheat grain milling. About 150 million tons are produced per year worldwide and its main use  
37 is as a low value component in animal food (Prückler et al., 2014). The general composition of  
38 wheat bran is as follows: water (12.1%), proteins (13.2 – 18.4%), fats (3.5 – 3.9%), starch (13.8  
39 – 24.9%), cellulose (11.0%), arabinoxylans (10.9 – 26.0%),  $\beta$ -glucans (2.1 – 2.5%), phenolic  
40 acids (0.02 – 1.5%) and ash (3.4 – 8.1%) (Apprich et al., 2014). Arabinoxylans (AXs) are a  
41 major component contained in the cell walls of wheat bran. AXs belong to the hemicellulosic  
42 part of biomass and are composed of a backbone of  $\beta$ -1,4 linked D-xylopyranosyl residues  
43 (Izydorczyk and Biliaderis, 2007). The abundance of arabinoxylans in wheat bran makes them  
44 susceptible to be extracted and converted into different platform molecules (furfural, succinic  
45 acid, xylitol, arabitol, among others) (Apprich et al., 2014).



46

47 Fig. 1. Conversion of arabinoxylans into high added-value products (Choudhary et al., 2013;  
 48 Kobayashi et al., 2011; Tathod et al., 2014; Zhang et al., 2012).

49 In general, hemicelluloses are partly solubilized and hydrolyzed during biomass fractionation,  
 50 resulting in an aqueous fraction enriched in hemicellulosic poly/oligosaccharides and in a solid  
 51 fraction with a high content in cellulose and lignin. Although hemicellulosic  
 52 poly/oligosaccharides have important applications in pharmaceutical and food industries, the  
 53 potential as platform molecules is larger for monomeric sugars. The reaction routes for the  
 54 production of different chemicals from arabinoxylans are shown in Fig. 1. Arabitol, xylitol and  
 55 succinic acid are found among the top 12 value-added products derived from biomass included  
 56 in the report published by the US Department of Energy (DOE). For example, arabitol and  
 57 xylitol are used as sugar substituents due to their low calorie content and also they are well

58 known for their anticariogenic properties (Koganti and Ju, 2013). Succinic acid has its main  
59 application as a C4 building block for fuel additives, solvents and biopolymers, among others  
60 (Choudhary et al., 2013).

61 Therefore, the fractionation and the complete hydrolysis of hemicellulosic poly/oligosaccharides  
62 into monomers are critical for an integrated biorefinery. Fractionation implies the selectively  
63 release of hemicelluloses from the biomass structure to the liquid medium. In a previous work, a  
64 hydrothermal fractionation assisted by heterogeneous catalysts was used, and their conditions  
65 were optimized (Sánchez-Bastardo et al., 2017). Hydrolysis of hemicelluloses is commonly  
66 carried out by two different methods: using mineral acids (hydrolysis yield: 50-89%) (Hilpmann  
67 et al., 2016; Kim et al., 2013; Kusema et al., 2013; Li et al., 2016; Nakasu et al., 2016) or  
68 enzymes (hydrolysis yield: 6-84%) (Jia et al., 2016; Lee et al., 2013; Li, Wang et al., 2016; Li,  
69 Xue et al., 2016; Lou et al., 2016; Moreira and Filho, 2016). Chemical hydrolysis using mineral  
70 acids is not an environmentally-friendly process. Although the acids themselves are such a  
71 cheap reagent, this process involves an increase in capital costs, as it requires corrosion resistant  
72 materials. Moreover, a precipitation with calcium ions to remove the acid is needed, what  
73 produces lime as a side product (Negahdar et al., 2016). The use of enzymes is a green process.  
74 Nevertheless, the long time required (several hours and even days), the nonexistence of  
75 recovery methods, the extremely high prize of enzymes and the critical control of reactions  
76 make necessary to look for other alternatives (Aden et al., 2002; Cará et al., 2013; Hendriks and  
77 Zeeman, 2009; Ormsby et al., 2012). Hydrolysis of hemicelluloses using solid acid catalysts  
78 appears as a green alternative to these methods. Operation times can be reduced and  
79 consequently the formation of degradation products and energy consumption. In the last 6 years,  
80 the development of solid acid catalysts applied to hydrolysis processes of hemicelluloses has  
81 attracted the interest of several authors (Cará et al., 2013; Dhepe and Sahu, 2010; Kusema et al,  
82 2011; Sahu and Dhepe, 2012; Salmi et al., 2014; Vilcocq et al., 2014; Zhou et al., 2013).  
83 Hydrolysis of polysaccharides over solid acid catalysts is a sequence of three first order  
84 reactions: 1) hydrolysis of polysaccharides into oligosaccharides, 2) hydrolysis of

85 oligosaccharides into monosaccharides, 3) depending on the reaction conditions, dehydration of  
86 monosaccharides into products such as furfural (Vilcocq et al., 2014). Different solid acid  
87 catalysts have been tested for hemicelluloses hydrolysis: zeolites, sulfonated resins, mesoporous  
88 silica materials, etc. Cará et al. (2013) reported a maximum hydrolysis yield of xylose +  
89 arabinose of 80% using Amberlyst 35 as solid catalyst and commercial beechwood xylan as raw  
90 material (120 °C, 10 bar argon, 4 hours). Dhepe et al. (2010) achieved a hydrolysis yield (xylose  
91 + arabinose) equal to 54% from oat spelt using zeolite HUSY (Si/Al=15) (170 °C, 2 h, 50 bar  
92 nitrogen). Kusema et al. (2011) used two different sulfonated resins to study the hydrolysis of  
93 commercial arabinogalactan. The highest yield they reported was 95% (monomeric arabinose)  
94 with Smopex-101 (pH=2) at 90 °C after 3 hours. Sahu et al. (2012) studied the effect of different  
95 solid acid catalysts on the oat spelt hydrolysis. They got a hydrolysis yield (xylose + arabinose)  
96 of 41% using zeolite HUSY (Si/Al=15) (170 °C, 3 h, 50 bar nitrogen). All these studies use  
97 commercial hemicelluloses as model compounds of real hemicelluloses contained in different  
98 types of biomass. However, only few studies are focused on the hydrolysis of hemicelluloses  
99 extracted directly from biomass (Vilcocq et al., 2014). The process starts with the fractionation  
100 of biomass to recover selectively the hemicellulosic fraction and complete the hydrolysis  
101 subsequently. When hemicelluloses are extracted from real biomass, the purity of the extracts is  
102 limited. Other compounds such as extractives, sugars, proteins and ash are also obtained  
103 together with the hemicelluloses. All these compounds can interfere in the efficiency of the  
104 hydrolysis process resulting in some limitations. Optimizing the hydrolysis step of a real  
105 mixture enriched in hemicelluloses is an issue of utmost importance for a concept of a  
106 biorefinery.

107 In this work, the heterogeneous catalytic hydrolysis of an extract enriched in arabinoxylans  
108 obtained from destarched wheat bran has been studied. Different experimental conditions, such  
109 as type and amount of catalyst and reaction time, have been tested in order to maximize the  
110 yield into monomers (xylose and arabinose) and minimize their further degradation into  
111 furfural.

112

## 113 2. Materials and Methods

### 114 2.1 Support and catalyst preparation

115 Synthesis of two mesoporous silica supports, MCM-48 and Al-MCM-48, was carried out using  
116 the procedure described by Romero et al. in a previous work (Romero et al., 2016). 2.0 g of n-  
117 hexadecyltrimethylammonium bromide (for molecular biology,  $\geq 99\%$ ; Sigma-Aldrich) were  
118 dissolved in 42 mL of distilled water, 18 mL of absolute ethanol (Panreac AppliChem) and 13  
119 mL of an aqueous ammonia solution (20% w·w<sup>-1</sup>) (Panreac AppliChem). After 15 minutes  
120 stirring, 0.077 g of sodium aluminate (technical, anhydrous; Sigma-Aldrich) were incorporated  
121 only for the Al-MCM-48 synthesis. Then, 4 mL of tetraethyl orthosilicate ( $\geq 99.0\%$  (GC);  
122 Sigma-Aldrich) were added dropwise and the solution was further stirred for 18 h. A white  
123 precipitate was formed and recovered by filtration while washing with distilled water. This  
124 precipitate was dried at 60 °C overnight. After drying, the samples were calcined to eliminate  
125 the surfactant applying a heating rate of 2 °C·min<sup>-1</sup> from 80 to 550 °C and maintained at 550 °C  
126 overnight.

127 Ruthenium or iron chloride catalysts were synthesized by wetness impregnation method using  
128 the so prepared MCM-48 or Al-MCM-48 as silica supports (Romero et al., 2016). Ruthenium  
129 (III) chloride (anhydrous; Strem Chemicals Inc.) or iron (III) chloride (reagent grade, 97%;  
130 Sigma-Aldrich) together with the corresponding support were suspended in water and sonicated  
131 for 10 minutes. This mixture was heated up from 30 to 80 °C with a heating rate of 1 °C·min<sup>-1</sup>  
132 and constant stirring. When water was evaporated, the resulting catalyst was dried overnight at  
133 105 °C to eliminate the remaining water.

### 134 2.2 Support and catalyst characterization

135 Nitrogen adsorption-desorption isotherms were performed with ASAP 2020 (Micromeritics,  
136 USA) to determine surface and pore properties of the catalysts. Before analysis, the samples  
137 were outgassed overnight at 350 °C. The multipoint BET method at  $P/P_0 \leq 0.3$  was used to  
138 calculate the total specific surface area. The total specific pore volume was evaluated from N<sub>2</sub>

139 uptake at  $P/P_0 \geq 0.99$  and the pore diameter was determined by BJH adsorption average ( $4 \cdot V \cdot A^{-1}$ , nm).

141 The ruthenium amount of the  $\text{RuCl}_3$ -based catalysts was determined by atomic absorption (AA)  
142 spectrophotometry (SPECTRA 220FS analyser) after a digestion of the samples with HCl,  $\text{H}_2\text{O}_2$   
143 and HF using microwave at 250 °C.

144 The acidity of the different supports and metal catalysts was estimated by titration with NaOH.  
145 This method is based on procedures already reported by several authors (Hu et al., 2015; Hu  
146 et al., 2016; Liu et al., 2013; Wang et al., 2011; Zheng et al., 2014).

### 147 2.3 Recovery of arabinoxylan fraction from wheat bran

148 A destarched wheat bran suspension ( $30 \text{ g} \cdot \text{L}^{-1}$ ) together with 500 mg of  $\text{RuCl}_3/\text{Al-MCM-48}$  was  
149 located in an extractor of 170 mL volume, made of AISI 304 stainless steel. The extraction was  
150 performed at 180 °C and autogenous pressure for 10 minutes under hot compressed water  
151 conditions. The optimization of these fractionation conditions is described in a previous work  
152 (Sánchez-Bastardo et al., 2017). After cooling, the final mixture was filtered to separate the  
153 remaining solid and the liquid extract enriched in arabinoxylans. This arabinoxylan extract,  
154 composed mainly by oligomers, was further subjected to the hydrolysis process itself. The  
155 composition of this extract that is indeed the raw material for the hydrolysis study is presented  
156 in Table 1.

### 157 2.4 Hydrolysis experiments

158 Hydrolysis experiments of the extract enriched in arabinoxylans were performed in a  
159 commercial stainless steel high pressure reactor (30 mL, Berghof BR-25) with a PID controller.  
160 First, the corresponding solid catalyst was placed inside the reactor. Once the reactor was  
161 closed, it was vented three times with nitrogen in order to eliminate the oxygen and heated up to  
162 the operating temperature (180 °C). When desired temperature was reached, the arabinoxylan  
163 solution preheated at 50 °C was pumped using a HPLC pump (PU-2080 Plus; Jasco). After  
164 pumping, temperature inside the reactor dropped to approximately 170 °C and initial time (0  
165 min) was considered when temperature reached again 180 °C (this lasts approximately 3 min).

166 At this moment, nitrogen pressure was adjusted to the operating pressure (50 bar). At the end of  
167 the experiments, the reaction was quenched by introducing the reactor in an ice-bath. The  
168 catalyst is recovered by filtration and the liquid was used for further analysis of monomeric  
169 sugars, degradation products and by-products. The amount of catalyst in each experiment is  
170 given as g of catalyst per g of C in initial hemicelluloses. However, in order to shorten, only g·g  
171 C<sup>-1</sup> appears along the text.

## 172 2.5 Initial and final products analysis

173 The identification and quantification of sugars and degradation products were done by High  
174 Performance Liquid Chromatography (HPLC).

175 The monosaccharides and degradation products were directly analyzed in the liquid samples.

176 However, for the total sugars determination in the initial solution (monomers and oligomers) an

177 acid hydrolysis pretreatment was used according to the Laboratory Analytical Procedure (LAP)

178 by NREL described by Sluiter et al. (2008). This method consisted of adding 0.8 mL of sulfuric

179 acid (72%) to 20 mL of the initial liquid sample. After the sample was autoclaved at 121 °C for

180 1 hour, calcium carbonate was added to get a pH between 5 and 6. An aliquot of 10 mL was

181 filtered (pore size 0.22 µm, Diameter 25 mm, Nylon; FILTER-LAB) and treated with 1 g of

182 mixed bed ion exchange resin (Dowex® Monosphere® MR-450 UPW; Sigma-Aldrich) to

183 remove all the ions before the HPLC analysis. All the samples were analyzed using a

184 chromatography system consisting of an isocratic pump (Waters 1515; Waters Corporation) and

185 an automatic injector (Waters 717; Waters Corporation). Two different HPLC columns were

186 used for the identification and quantification of the different products in the liquid samples:

187 1) Supelcogel Pb (Supelco) for sugars (milli-Q water as mobile phase, 0.5 mL·min<sup>-1</sup> as flow rate

188 and 85 °C as temperature) and 2) Sugar SH-1011 (Shodex) for degradation products (sulfuric

189 acid 0.01 N as mobile phase, 0.8 mL·min<sup>-1</sup> as flow rate and 50 °C as temperature). Sugars and

190 acids were identified using an IR detector (Waters 2414; Waters Corporation). 5-

191 hidroxymethylfurfural (5-HMF) and furfural were determined with an UV-Vis detector (Waters

192 2487; Waters Corporation) at a wavelength of 254 and 260 nm, respectively. The standards



193 employed for the HPLC analysis were: cellobiose (98%), glucose (99%), xylose (99%),  
 194 galactose (99%), arabinose (99%), mannose (99%), fructose (99%), glyceraldehyde (95%),  
 195 glycolaldehyde (99%), lactic acid (85%), formic acid (98%), acetic acid (99%), levulinic acid  
 196 (98%), acrylic acid (99%), pyruvaldehyde (40%), 5-hydroxymethylfurfural (99%) and furfural  
 197 (99%). All these chemicals were purchased from Sigma-Aldrich (Spain) and used as received.  
 198 The hydrolysis yield of arabinose and xylose oligomers into arabinose and xylose, respectively,  
 199 and the total arabinoxylan hydrolysis yield were calculated as follows (Eq. 1-3):

$$\% \text{ Ara hydrolysis yield} = \frac{\text{Ara as monomeric sugar in hydrolyzed liquid (g)}}{\text{Ara as total sugars}^a \text{ in initial liquid extract (g)}} \times 100 \quad (\text{Eq. 1})$$

$$\% \text{ Xyl hydrolysis yield} = \frac{\text{Xyl as monomeric sugar in hydrolyzed liquid (g)}}{\text{Xyl as total sugars}^a \text{ in initial liquid extract (g)}} \times 100 \quad (\text{Eq. 2})$$

$$\% \text{ AX hydrolysis yield} = \frac{(\text{Ara+Xyl}) \text{ as monomeric sugar in hydrolyzed liquid (g)}}{(\text{Ara+Xyl}) \text{ as total sugars}^a \text{ in initial liquid extract (g)}} \times 100 \quad (\text{Eq. 3})$$

200 Ara: Arabinose, Xyl: Xylose

201 <sup>a</sup> Total sugars refer to the sum of the corresponding sugars (arabinose and/or xylose) as monomers plus  
 202 oligomers

### 203 3. Results and Discussion

#### 204 3.1 Composition of initial arabinoxylan extract

205 The composition of the enriched arabinoxylan extract obtained from wheat bran and used in the  
 206 hydrolysis experiments is given in Table 1. Table 1 presents the amount of each sugar which is  
 207 in monomeric and oligomeric form respect the total amount of the corresponding sugar. In the  
 208 case of arabinose, practically 50% percent is already in monomeric form after the fractionation  
 209 process, whereas 95% of the xylose appears as oligosaccharide.

210 The initial total amount of arabinose and xylose (monomers + oligomers) expressed in g·L<sup>-1</sup> is  
 211 3.1 and 6.2, respectively. This means that these are the maximum values which both sugars can  
 212 reach after the hydrolysis process.

213

214

215 Table 1. Chemical composition of the initial extract.

Compound			
Proteins <sup>a</sup> (mg/L)	1676 ± 113		
Sugars	Monomeric sugars (mg/L)	Oligomeric sugars (mg/L)	% Olig <sup>b</sup>
Glc	195 ± 32	1609 ± 197	89
Xyl	284 ± 9	5944 ± 188	95
Gal	82 ± 26	255 ± 34	76
Ara	1522 ± 112	1605 ± 34	51
Man	70 ± 9	2 ± 44	2

216 <sup>a</sup> Proteins were determined following a standardized Kjeldahl method using a nitrogen to protein conversion factor of  
217 5.7 applicable to wheat bran

218 <sup>b</sup> %Olig. = percentage of each sugar in oligomeric form: g of each oligomeric sugar/g of the total corresponding sugar  
219 x 100

### 220 3.2 Catalyst characterization

221 The properties of the different solid catalysts used in this work are summarized in Table 2.

222 Specific surface area, total pore volume, pore diameter and acidity values were determined.

223 MCM-48 and Al-MCM-48 have specific surface areas of 1298 and 1352 m<sup>2</sup>·g<sup>-1</sup>, and pore

224 volumes of 0.87 and 0.81 cm<sup>3</sup>·g<sup>-1</sup>, respectively. According to these results, no significant

225 changes in surface area and pore volume were observed between these two mesoporous

226 materials. Pore diameter was slightly higher for Al-MCM-48 (2.5 nm) than for MCM-48 (2.2

227 nm). After RuCl<sub>3</sub> or FeCl<sub>3</sub> impregnation, a decrease in the specific surface area and pore volume

228 was detected. This fact can be attributed to the partial blocking of the porous network in

229 mesoporous supports. After RuCl<sub>3</sub> deposition on MCM-48, no changes in the pore size were

230 appreciated. However, pore size slightly increased from 2.5 to 2.7 nm and 2.6 nm after

231 deposition of RuCl<sub>3</sub> and FeCl<sub>3</sub>, respectively, on Al-MCM-48. This indicates slender

232 modifications of pore structure, suggesting a higher pore blocking in Al-MCM-48 supported

233 catalysts than in MCM-48 catalysts. Ruthenium and iron content for RuCl<sub>3</sub> and FeCl<sub>3</sub>-based

234 catalysts was around 4% in both cases, determined by AA.

235 Acidity is a key parameter of catalysts for hydrolysis reactions. The acidity of the catalysts used

236 in this work presents the following trend: MCM-48 < Al-MCM-48 < RuCl<sub>3</sub>/MCM-48 <

237 RuCl<sub>3</sub>/Al-MCM-48 < FeCl<sub>3</sub>/Al-MCM-48.

238 Table 2. Structural characterization of solid catalysts.

Catalyst	Metal content (%)	S <sub>BET</sub> (m <sup>2</sup> ·g <sup>-1</sup> )	V <sub>pore</sub> <sup>a</sup> (cm <sup>3</sup> ·g <sup>-1</sup> )	D <sub>pore</sub> <sup>b</sup> (nm)	Acidity (mEq H <sup>+</sup> ·g cat. <sup>-1</sup> )
MCM-48	-	1298	0.87	2.2	0.293
Al-MCM-48	-	1352	0.81	2.5	0.598
RuCl <sub>3</sub> /MCM-48	4.1	1032	0.63	2.2	0.738
RuCl <sub>3</sub> /Al-MCM-48	4.3	1018	0.63	2.7	1.130
FeCl <sub>3</sub> /Al-MCM-48	4.2	1018	0.59	2.6	1.429

239 <sup>a</sup> Total specific pore volume was evaluated from N<sub>2</sub> uptake at  $P/P_0 \geq 0.99$

240 <sup>b</sup> Pore diameter was determined by BJH adsorption average

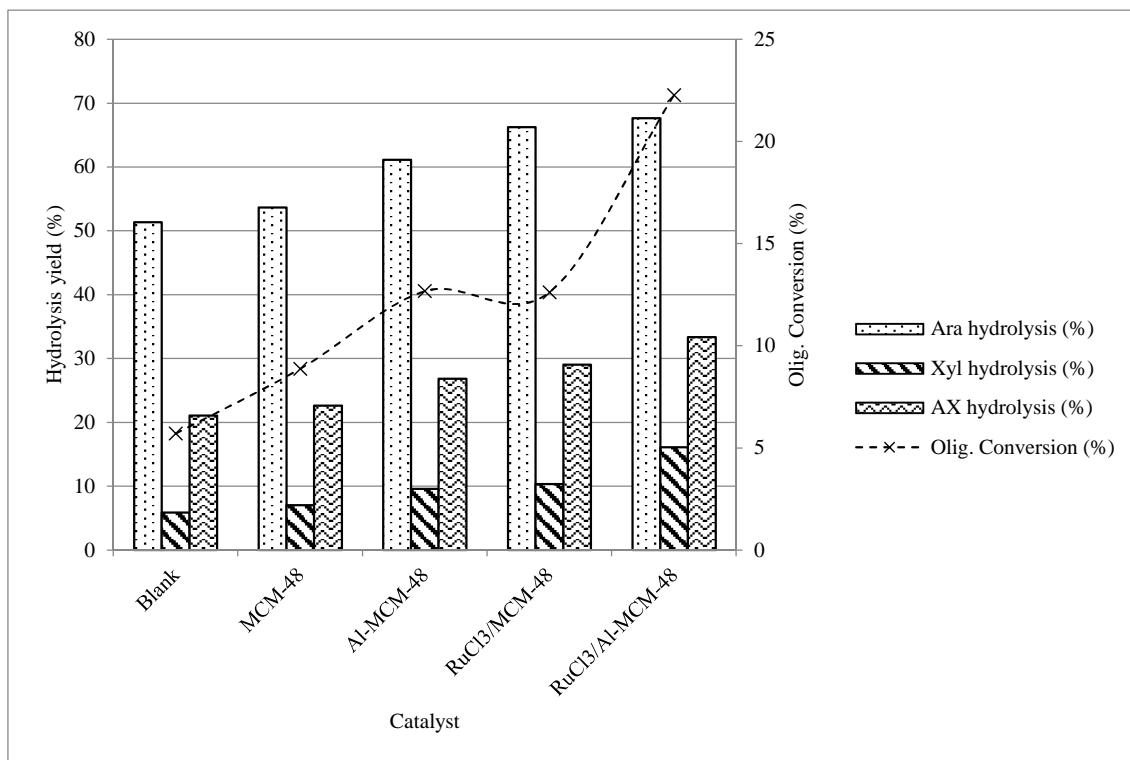
### 241 3.3 Arabinoxylan hydrolysis experiments

242 The effect of different parameters (type and amount of catalyst, reaction time and different  
 243 metal cations) was studied in the hydrolysis of an arabinoxylan enriched extract obtained from  
 244 destarched wheat bran. The results are discussed in terms of hydrolysis yield of arabinose and  
 245 xylose oligomers. The formation of furfural, as the main degradation product derived from  
 246 dehydration of arabinose and xylose, was also taken into account.

#### 247 3.3.1 Effect of different mesoporous silica materials and RuCl<sub>3</sub> based-catalysts

248 A first screening of different mesoporous silica supports and the corresponding RuCl<sub>3</sub> based-  
 249 catalysts was carried out. MCM-48, Al-MCM-48, RuCl<sub>3</sub>/MCM-48 and RuCl<sub>3</sub>/Al-MCM-48 were  
 250 tested in the arabinoxylan hydrolysis (Fig. 2). The experimental conditions were 180 °C, 15  
 251 minutes and 50 bar N<sub>2</sub>. The ratio of catalyst to carbon content in hemicelluloses of the initial  
 252 extract was 0.6 g·g<sup>-1</sup>, which is the same ratio used in the previous fractionation from wheat bran.  
 253 The trend observed in total AX hydrolysis yield is as follows: Blank ≈ MCM-48 < Al-MCM-48  
 254 < RuCl<sub>3</sub>/MCM-48 < RuCl<sub>3</sub>/Al-MCM-48. This is in agreement with the acidity values of  
 255 catalysts: higher acidities result in higher hydrolysis yields. In the absence of catalyst (blank  
 256 reaction), the amount of monomeric arabinose and xylose turns out to be the same as in the  
 257 initial AX solution (Table 1). At 180 °C, the pK<sub>w</sub> of water is low, which means that the amount  
 258 of protons derived from water is relatively high (Bandura and Lvov, 2006). However, as it is  
 259 shown in Fig. 2, the water protonation is not enough to cause the breakdown of arabinoxylan  
 260 molecules into monomers under these conditions. MCM-48 is the least acidic catalyst and its  
 261 surface acidity is due to silanol groups (Si – OH), which correspond to weak acid sites (Xue et.,

262 2004). The weak nature of these sites does not practically improve AX hydrolysis, although a  
263 slight increase in arabinose oligomers hydrolysis is observed. Al-MCM-48 exhibits a higher  
264 catalytic activity in this hydrolysis process. Specially, Al-MCM-48 improves the conversion of  
265 arabinose oligomers into monomers. During Al-MCM-48 synthesis, a silicon atom ( $\text{Si}^{+4}$ ) is  
266 replaced by an aluminum atom ( $\text{Al}^{+3}$ ) in a tetrahedral network. Thus, a cation, usually a proton,  
267 is required to balance the aluminum tetrahedron. This compensation proton derives in a  
268 Brønsted acid site, which increases the total acidity of the Al-MCM-48 (Kao et al., 2008). In Al-  
269 MCM-48, Brønsted acidity is higher than Lewis acidity due to the large amount of  
270 tetraordinated aluminum on the silica surface (Krithiga et al., 2005).  $\text{RuCl}_3$  supported  
271 catalysts ( $\text{RuCl}_3/\text{MCM-48}$  and  $\text{RuCl}_3/\text{Al-MCM-48}$ ) demonstrated to be more active in AXs  
272 hydrolysis than the corresponding mesoporous silica materials (MCM-48 and Al-MCM-48,  
273 respectively). Higher activity of  $\text{RuCl}_3$  catalysts in hydrolysis reactions is related to their global  
274 acidity.  $\text{RuCl}_3$ -based catalysts show higher acidity than the corresponding mesoporous silica  
275 support, which is due to the high acidity of  $\text{RuCl}_3$  (Guisnet et al., 1993). In addition to this,  
276 several authors have already reported that cations with moderate Lewis acidity, such as  $\text{Ru}^{+3}$ ,  
277 are found to be active in hydrolysis of cellobiose or cellulose (Jing et al., 2016; Shimizu et al.,  
278 2009). In all the cases, furfural formation was negligible in comparison to the amount of  
279 arabinose and xylose.



280

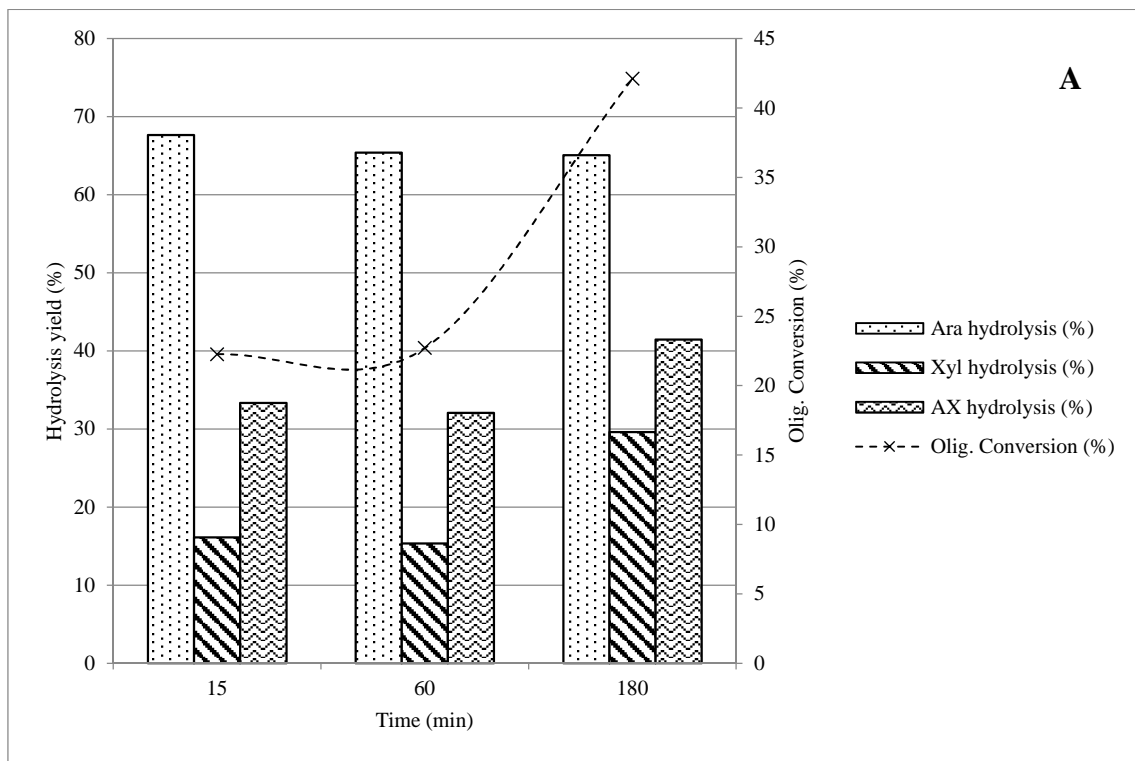
281 Fig. 2. Comparison of different catalysts in arabinoxylan hydrolysis yield and oligomers  
 282 conversion. Reaction conditions: 180 °C, 50 bar N<sub>2</sub>, 15 min, 0.6 g catalyst·g C<sup>-1</sup> in initial  
 283 hemicelluloses.

284 Although it has been shown that a more acidic catalyst leads to a higher conversion of AXs into  
 285 monomeric sugars, hydrolysis yields and oligomer conversion under these experimental  
 286 conditions were still very low. RuCl<sub>3</sub>/Al-MCM-48, as the most active catalyst, was chosen for a  
 287 further study to improve hydrolysis yield.

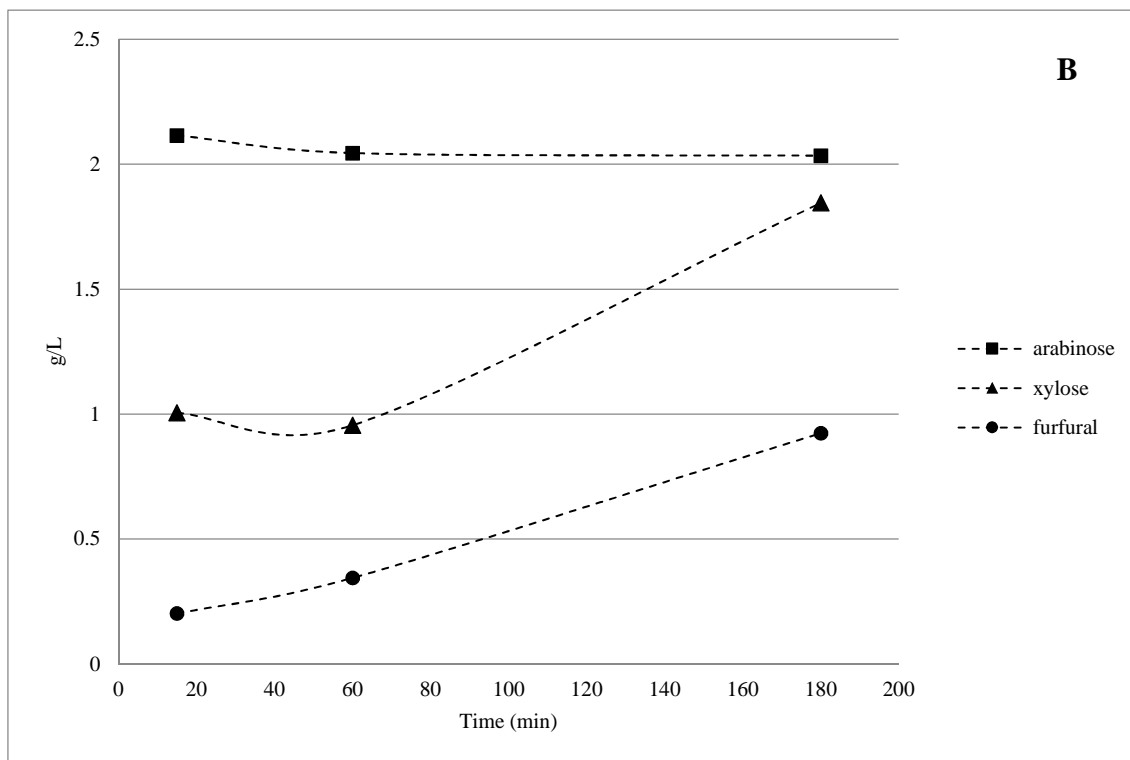
### 288 3.3.2 Effect of catalyst amount and reaction time

289 RuCl<sub>3</sub> supported on mesoporous Al-MCM-48 was used to study the influence of reaction time  
 290 and catalyst loading on hydrolysis yield. First, a low amount of catalyst (0.6 g·g C<sup>-1</sup>) was tested  
 291 at 180 °C, 50 bar N<sub>2</sub> and different reaction times (15-180 min) (Fig. 3). A maximum of 68% in  
 292 the hydrolysis yield of arabinose oligomers is achieved at 15 minutes of reaction, as a  
 293 consequence of their degradation into furfural for longer times. No difference is observed in  
 294 terms of arabino-oligosaccharides hydrolysis yield for times beyond 15 minutes. However, with  
 295 this low amount of catalyst, the maximum hydrolysis yield of xylose oligomers is obtained after

296 180 minutes of reaction, where the concentration of furfural becomes also important due to  
 297 xylose degradation, as it is shown in Fig. 3B. This means that monomeric xylose is slowly  
 298 formed and partially degraded into furfural after 3 hours. Part of xylose obtained over time has  
 299 had probably enough time to be converted into furfural. At short times, xylose detected is low  
 300 because xylose oligomers have not been hydrolyzed. At longer times, this amount is higher but  
 301 hydrolysis yield of xylose oligomers is still low ( $\approx 30\%$ ) due to the slow xylose formation from  
 302 xylo-oligosaccharides and fast degradation into furfural. The large quantity of furfural also  
 303 evidences the slow hydrolysis rate of xylose oligomers into xylose compared to the high  
 304 degradation rate of xylose into furfural.



305

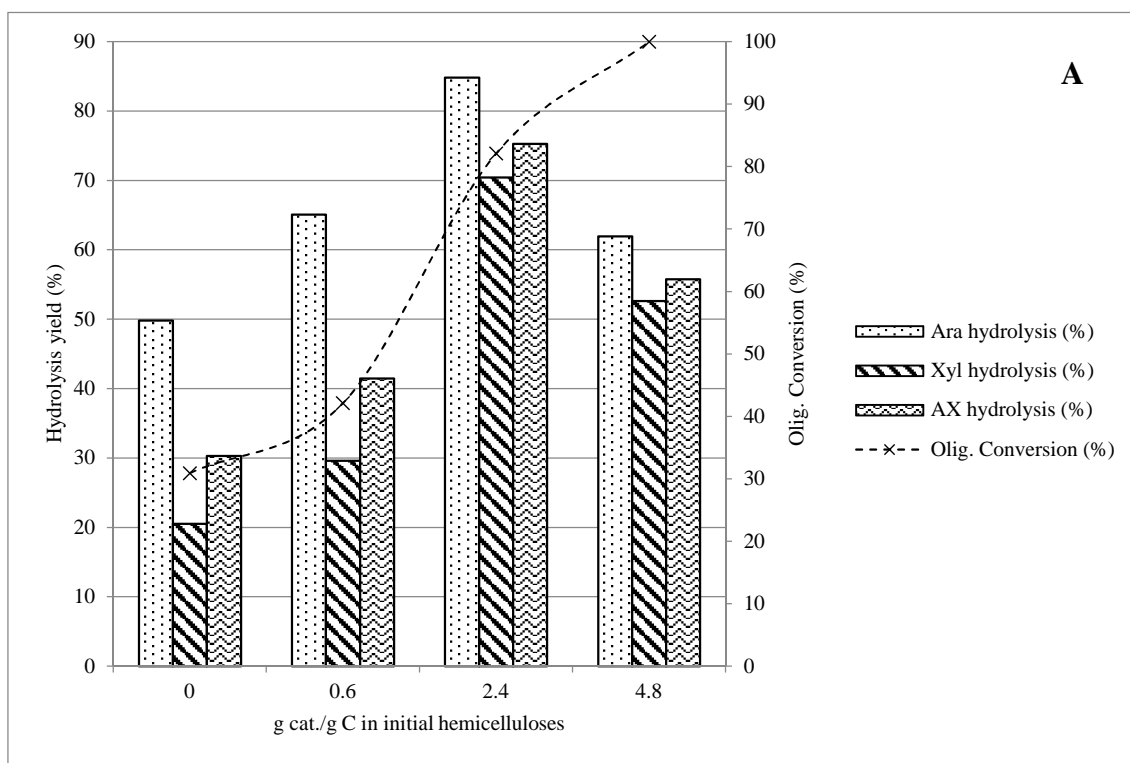


306

307 Fig. 3. Effect of time in arabinoxylan hydrolysis with low amount of catalyst. Reaction  
 308 conditions: 180 °C, 50 bar N<sub>2</sub>, catalyst: RuCl<sub>3</sub>/Al-MCM-48, catalyst loading: 0.6 g catalyst·g C<sup>-1</sup>  
 309 in initial hemicelluloses. A) Hydrolysis yield and oligomers conversion, B) Composition of the  
 310 liquid after hydrolysis (g·L<sup>-1</sup>).

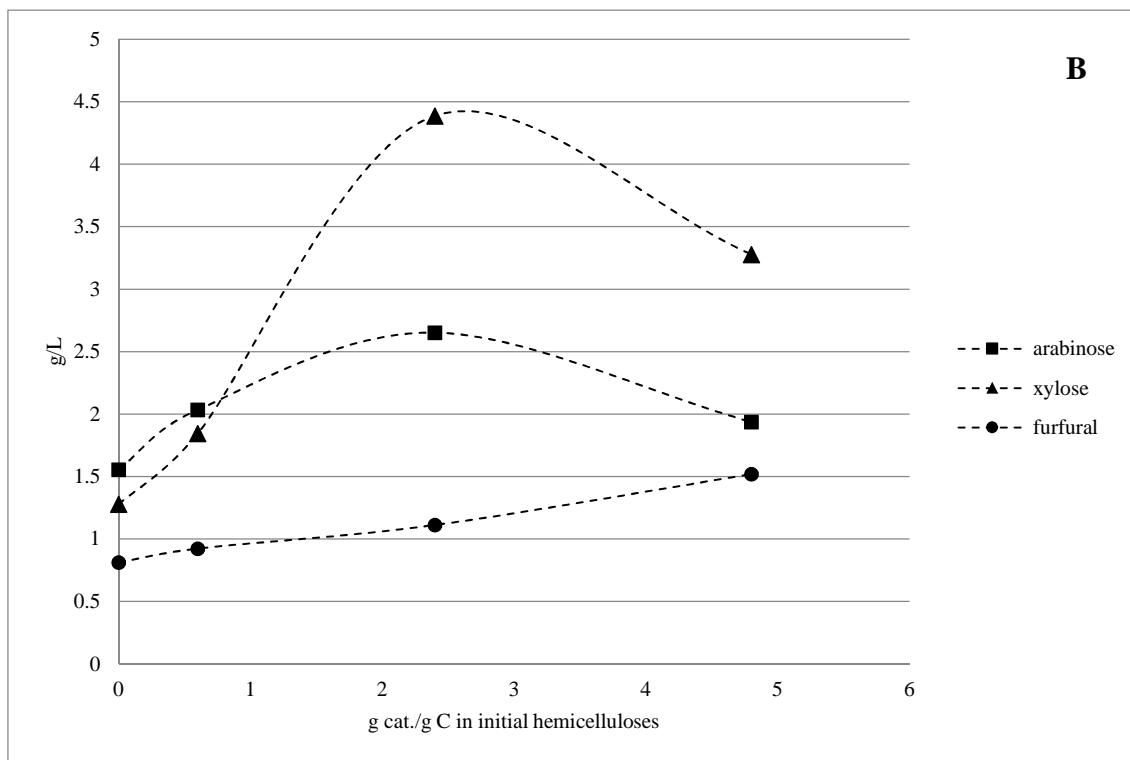
311 To overcome this degradation is necessary to speed up the xylo-oligosaccharides hydrolysis step  
 312 but inhibiting further degradation. Three different amounts of catalyst (0.6, 2.4 and 4.8 g·g C<sup>-1</sup>)  
 313 were tested at 180 °C and 3 hours under 50 bar of N<sub>2</sub> (Fig. 4). The hydrolysis yield of xylose  
 314 oligomers reaches 70% after 3 hours with a catalyst loading of 2.4 g·g C<sup>-1</sup>. Under these  
 315 conditions, the hydrolysis yield of arabino-oligosaccharides is already 85%. When catalyst  
 316 loading is increased from 0.6 to 2.4 g·g C<sup>-1</sup>, monomeric xylose and arabinose in the liquid after  
 317 hydrolysis rise in a greater proportion than furfural. This means that arabinose and xylose  
 318 formation is faster than the consecutive degradation into furfural. This was also observed and  
 319 well explained by Sahu et al. (2012). They studied the effect of substrate/catalyst ratio on  
 320 hemicelluloses hydrolysis using HUSY zeolite as catalyst. Interactions between the substrate  
 321 (hemicelluloses) and available active sites in catalyst decrease as increasing substrate/catalyst

322 ratio (decreasing catalyst amount); in addition to this, once xylose is formed, it may undergo  
 323 non-catalytic degradation reactions. In that work, a xylose+arabinose yield of 35% was reported  
 324 when substrate/catalyst ratio was 130. However, when this ratio was 10, the yield of  
 325 arabinose+xylose was 56%. They concluded that the reaction rate of hemicelluloses into xylose  
 326 was higher than xylose to furfural when the amount of catalyst was increased. In the present  
 327 work, when catalyst loading was further increased (from 2.4 to 4.8 g·g C<sup>-1</sup>), the oligomer  
 328 conversion was total. However, after 3 hours of hydrolysis, a dramatic decrease in xylose and  
 329 arabinose is observed and black sediment appears. This black sediment corresponds probably to  
 330 humins derived from furfural: arabinose and xylose are degraded to furfural and this later to  
 331 humins; that explains a drop in arabinose and xylose but not a sharp increase in furfural as it is  
 332 shown in Fig. 4B.



333



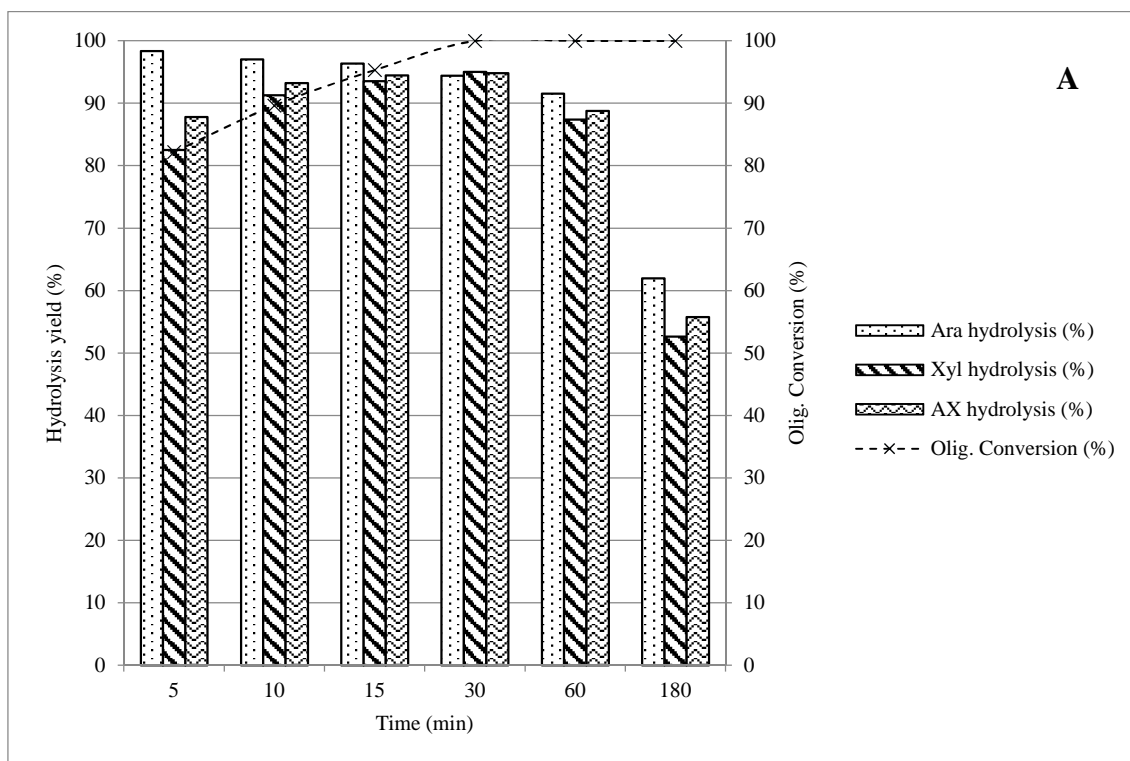


334

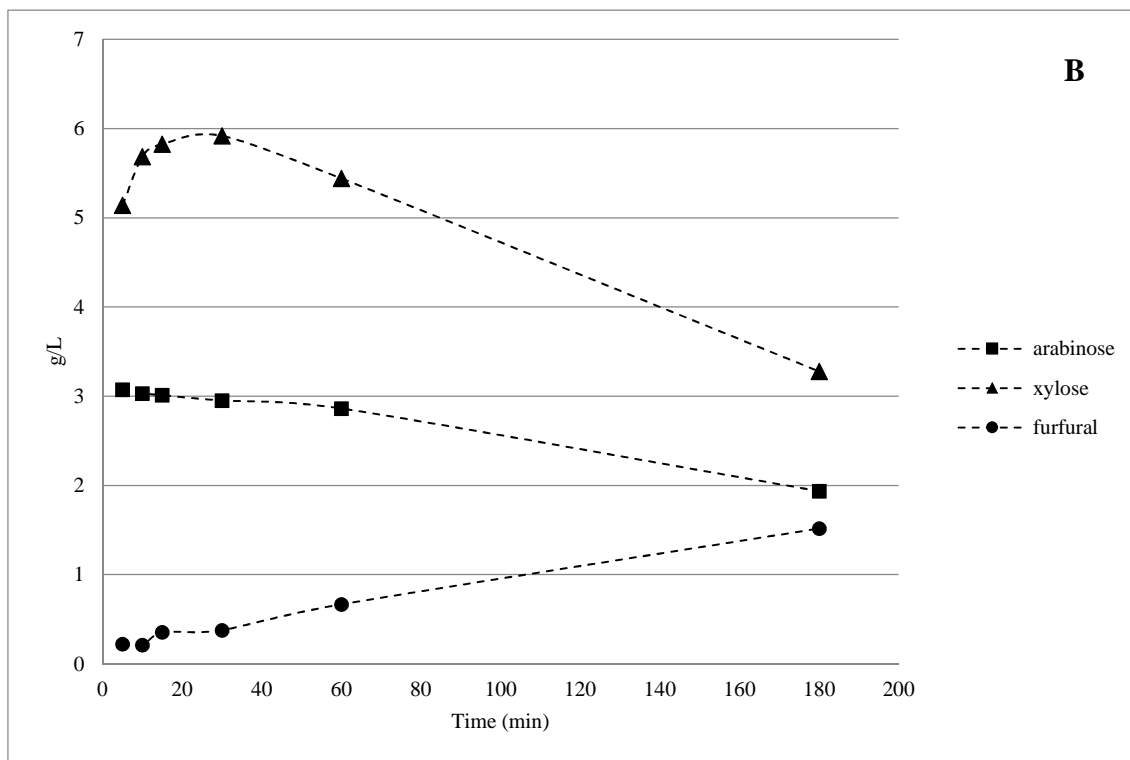
335 Fig. 4. Effect of the amount of catalyst in arabinoxylan hydrolysis. Reaction conditions: 180 °C,  
 336 3 h, 50 bar N<sub>2</sub>, catalyst: RuCl<sub>3</sub>/Al-MCM-48. A) Hydrolysis yield of arabinoxylans and  
 337 oligomers conversion, B) Composition of the liquid after hydrolysis (g·L<sup>-1</sup>).

338 In order to shorten reaction times and subsequent degradation, the highest catalyst loading (4.8  
 339 g·g C<sup>-1</sup>) was tested at shorter times (< 180 min) (Fig. 5). The hydrolysis yield of arabinose  
 340 oligomers is almost complete after 5 minutes (98%). Longer times make arabinose degrade  
 341 slowly into furfural. The hydrolysis of xylose oligomers gets the maximum yield after 15-30  
 342 minutes (94-95%), and then xylose starts to be degraded. Total conversion of oligomers is  
 343 reached after 15 minutes. The amount of furfural obtained rises after 30 minutes, due to  
 344 arabinose and xylose degradation. The hydrolysis of arabinose oligomers is always higher than  
 345 that of xylose. Arabinose side chains are linked by α-glycosidic bonds, whereas xylose units  
 346 from the backbone are connected by means of β-glycosidic bonds. α-glycosidic bonds are more  
 347 easily hydrolysable than β-glycosidic linkages, what explains the faster release of arabinose  
 348 molecules than xylose. This is well reported by Negahdar et al. (2016).

349 In conclusion, a high arabinoxylan hydrolysis yield was achieved at 180 °C, 15 minutes and 50  
 350 bar N<sub>2</sub> with a catalyst loading of 4.8 g·g C<sup>-1</sup>. Arabinose and xylose oligomers hydrolysis yields  
 351 were 96 and 94%, respectively. Under these conditions, the process is optimized since xylose  
 352 and arabinose reach practically the maximum amount possible. Moreover, the amount of  
 353 furfural was negligible in comparison to arabinose and xylose.



354



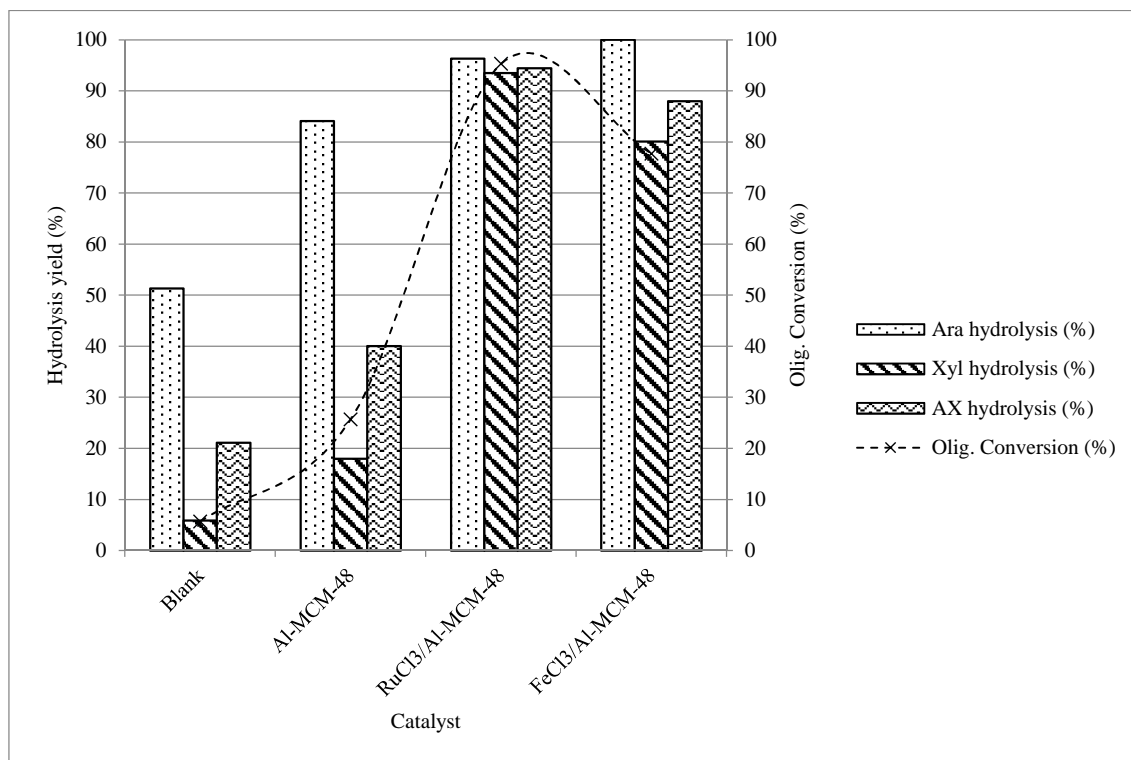
355

356 Fig. 5. Effect of time with high amount of catalyst in arabinoxylan hydrolysis. Reaction  
 357 conditions: 180 °C, 50 bar N<sub>2</sub>, catalyst: RuCl<sub>3</sub>/Al-MCM-48, catalyst loading: 4.8 g catalyst·g C<sup>-1</sup>  
 358 in initial hemicelluloses. A) Hydrolysis yield of arabinoxylans into arabinose and xylose and  
 359 oligomers conversion, B) Composition of the liquid after hydrolysis (g·L<sup>-1</sup>).

### 360 3.3.3 Effect of cation (Ru<sup>+3</sup>, Fe<sup>+3</sup>)

361 The effect of different cations (Ru<sup>+3</sup>, Fe<sup>+3</sup>) was studied using RuCl<sub>3</sub> and FeCl<sub>3</sub> supported on Al-  
 362 MCM-48 as catalysts. Experiments were performed at 180 °C, 15 minutes and 50 bar N<sub>2</sub> using  
 363 4.8 g·g C<sup>-1</sup>, which was optimized in previous sections. For comparison, a reaction with bare Al-  
 364 MCM-48 was also carried out to point out the effect of the metal precursors. Results are shown  
 365 in Fig. 6. It can be clearly seen that the incorporation of RuCl<sub>3</sub> or FeCl<sub>3</sub> enhances arabinoxylan  
 366 hydrolysis. The hydrolysis of arabinose oligomers is almost complete with both supported  
 367 catalysts. However, a higher hydrolysis yield of xylose oligomers is obtained with RuCl<sub>3</sub>-  
 368 catalyst, despite the greater acidity of FeCl<sub>3</sub>/Al-MCM-48 (Table 2). Fe<sup>+3</sup> and Ru<sup>+3</sup> have been  
 369 demonstrated to be active in hydrolysis of cellobiose and cellulose (Jing et al., 2016; Shimizu et  
 370 al., 2009). Nevertheless, higher reaction rates were observed for catalysts with moderate Lewis

371 acidity, such as  $\text{Ru}^{+3}$ , than for those with high Lewis acidity, such as  $\text{Fe}^{+3}$ . This could explain  
372 the better catalytic activity of  $\text{RuCl}_3$  catalysts in comparison with  $\text{FeCl}_3$  in arabinoxylan  
373 hydrolysis (Shimizu et al., 2009).



374

375 Fig. 6. Effect of cation ( $\text{Ru}^{+3}$ ,  $\text{Fe}^{+3}$ ) in arabinoxylan hydrolysis and oligomers conversion.  
376 Reaction conditions: 180 °C, 15 min, 50 bar  $\text{N}_2$ , catalyst loading: 4.8 g catalyst·g  $\text{C}^{-1}$  in initial  
377 hemicelluloses.

#### 378 4. Conclusions

379 The use of heterogeneous catalysts has been demonstrated to be a good option for hydrolysis of  
380 real arabinoxylans derived from wheat bran. The hydrolysis yield is improved by increasing the  
381 acidity of the heterogeneous catalyst (MCM-48 < Al-MCM-48 <  $\text{RuCl}_3/\text{MCM-48}$  <  $\text{RuCl}_3/\text{Al-}$   
382 MCM-48). Cations with moderate Lewis acidity ( $\text{Ru}^{+3}$ ) present a higher activity in hydrolysis  
383 processes than those with high Lewis acidity ( $\text{Fe}^{+3}$ ). In this work, a high hydrolysis yield of  
384 arabinoxylans into the corresponding monomers (94 and 96% for xylose and arabinose,  
385 respectively) is achieved at 180 °C after 15 minutes using an amount of  $\text{RuCl}_3/\text{Al-MCM-48}$   
386 equal to 4.8 g·g<sup>-1</sup>.

**387 Acknowledgements**

**388** Authors gratefully acknowledge the financial support of Spanish Government through the  
**389** Research Project CTQ2015-64892-R (MINECO/FEDER). N. Sánchez-Bastardo thanks  
**390** Ministerio de Educación Cultura y Deporte for financial support through a FPU predoctoral  
**391** contract (FPU14/00812).

## **392 References**

- 393** Aden, A., Ruth, M., Ibsen, K., Jechura, J., Neeves, K., Sheehan, J., Wallace, B., Montague, L.,  
**394** Slayton, A., Lukas, J., 2002. Lignocellulosic biomass to ethanol process design and economics  
**395** utilizing co-current dilute acid prehydrolysis and enzymatic hydrolysis for corn stover,  
**396** NREL/TP-510-32438.
- 397** Apprich, S., Tirpanalan, Ö., Hell, J., Reisinger, M., Böhmendorfer, S., Siebenhandl-Ehn, S.,  
**398** Novalin, S., Kneifel, W., 2014. Wheat bran-based biorefinery 2: Valorization of products. *LWT*  
**399** *Food Sci. Technol.* 56, 222-231.
- 400** Bandura, A.V., Lvov, S.N., 2006. The ionization constant of water over wide ranges of  
**401** temperature and density. *J. Phys. Chem. Ref. Data.* 35, 14-30.
- 402** Cará, P. D., Pagliaro, M., Elmekawy, A., Brown, D. R., Verschuren, P., Shiju, N. R.,  
**403** Rothenberg, G., 2013. Hemicellulose hydrolysis catalysed by solid acids. *Catal. Sci. Technol.* 3,  
**404** 2057-2061.
- 405** Choudhary, H., Nishimura, S., Ebitani, K., 2013. Metal-free oxidative synthesis of succinic acid  
**406** from biomass-derived furan compounds using a solid acid catalyst with hydrogen peroxide.  
**407** *Appl. Catal., A.* 458, 55-62.
- 408** Dhepe, P. L., Sahu, R., 2010. A solid-acid-based process for the conversion of hemicellulose.  
**409** *Green Chem.* 12, 2153-2156.
- 410** Guisnet, M., Barbier, J., Barrault, J., Bouchoule, C., Duprez, D., Pérot, G., Montassier, C.,  
**411** 1993. *Studies in Surface Science and Catalysis. Heterogeneous Catalysis and Fine Chemicals*  
**412** III. 1<sup>st</sup> Ed. Poitiers: Elsevier Science, 78, 1-719. Print ISBN 9780444890634.
- 413** Hendriks, A. T. W. M., Zeeman, G., 2009. Pretreatments to enhance the digestibility of  
**414** lignocellulosic biomass. *Bioresour. Technol.* 100, 10-18.

- 415 Hilpmann, G., Becher, N., Pahner, F-A., Kusema, B., Mäki-Arvela, P., Lange, R., Murzin, D.  
416 Y., Salmi, T., 2016. Acid hydrolysis of xylan. *Catal. Today.* 259, 376-380.
- 417 Hu, H., Li, Z., Wu, Z., Lin, L., Zhou, S., 2016. Catalytic hydrolysis of microcrystalline and rice  
418 straw-derived cellulose over a chlorine-doped magnetic carbonaceous solid acid. *Ind. Crops*  
419 *Prod.* 84, 408-417.
- 420 Hu, L., Tang, X., Wu, Z., Lin, L., Xu, J., Xu, N., Dai, B., 2015. Magnetic lignin-derived  
421 carbonaceous catalyst for the dehydration of fructose into 5-hydroxymethylfurfural in  
422 dimethylsulfoxide. *Chem. Eng. J.* 263, 299-308.
- 423 Izydorczyk, M.S., Biliaderis, C.G., 2007. Arabinoxylans: Technologically and nutritionally  
424 functional plant polysaccharides, in: Biliaderis, C. G., Izydorczyk, M. S. (Eds.), *Functional food*  
425 *carbohydrates*. Boca Raton: CRC Press, pp. 249-290.
- 426 Jia, L., Budinova, G. A. L. G., Takasugi, Y., Noda, S., Tanaka, T., Ichinose, H., Goto, M.,  
427 Kamiya, N., 2016. Synergistic degradation of arabinoxylan by free and immobilized xylanases  
428 and arabinofuranosidase. *Biochem. Eng. J.* 114, 268-275.
- 429 Jing, S., Cao, X., Zhong, L., Peng, X., Zhang, X., Wang, S., Sun, R., 2016. In situ carbonic acid  
430 from CO<sub>2</sub>: A green acid for highly effective conversion of cellulose in the presence of Lewis  
431 acid. *ACS Sustainable Chem. Eng.* 4, 4146-4155.
- 432 Kao, H-M., Chang, P-C., Liao, Y-W., Lee, L-P., Chien, C-H., 2008. Solid-state NMR  
433 characterization of the acid sites in cubic mesoporous Al-MCM-48 materials using  
434 trimethylphosphine oxide as a P NMR probe. *Microporous Mesoporous Mater.* 114, 352-364.
- 435 Kim, Y., Kreke, T., Ladisch, M. R., 2013. Reaction mechanisms and kinetics of xylo-  
436 oligosaccharide hydrolysis by dicarboxylic acids. *AIChE Journal.* 59, 188-199.

- 437 Kobayashi, H., Komanoya, T., Guha, S.K., Hara, K., Fukuoka, A., 2011. Conversion of  
438 cellulose into renewable chemicals by supported metal catalysis. *Appl. Catal., A.* 409-410, 13-  
439 20.
- 440 Koganti, S., Ju, L-K., 2013. *Debaryomyces hansenii* fermentation for arabitol production.  
441 *Biochem. Eng. J.* 79, 112-119.
- 442 Krithiga, T., Vinu, A., Ariga, K., Arabindoo, B., Palanichamy, M., Murugesan, V., 2005.  
443 Selective formation 2,6-diisopropyl naphthalene over mesoporous Al-MCM-48 catalysts. *J.*  
444 *Mol. Catal. A: Chem.* 237, 238-245.
- 445 Kusema, B. T., Hilmann, G., Mäki-Arvela, P., Willför, S., Holmbom, B., Salmi, T., Murzin, D.  
446 Y., 2011. Selective hydrolysis of arabinogalactan into arabinose and galactose over  
447 heterogeneous catalysts. *Catal. Lett.* 141, 408-412.
- 448 Kusema, B. T., Tönnov, T., Mäki-Arvela, P., Salmi, T., Willför, S., Holmbom, B., Murzin, D.  
449 Y., 2013. Acid hydrolysis of O-acetyl-galactoglucomannan. *Catal. Sci. Technol.* 3, 116-122.
- 450 Lee, H. J., Kim, I. J., Kim, J. F., Choi, I-G., Kim, K. H., 2013. An expansin from the marine  
451 bacterium *Hahella chejuensis* acts synergistically with xylanase and enhances xylan hydrolysis.  
452 *Bioresour. Technol.* 149, 516–519.
- 453 Li, F., Wang, H., Xin, H., Cai, J., Fu, Q., Jin, Y., 2016. Development, validation and application  
454 of a hydrophilic interaction liquid chromatography-evaporative light scattering detection based  
455 method for process control of hydrolysis of xylans obtained from different agricultural wastes.  
456 *Food Chem.* 212, 155-161.
- 457 Li, H., Xue, Y., Wu, J., Wu, H., Qin, G.; Li, C., Ding, J., Liu, J., Gan, L., Long, M., 2016.  
458 Enzymatic hydrolysis of hemicelluloses from *Miscanthus tomonosaccharides* or xylo-  
459 oligosaccharides by recombinant hemicellulases. *Ind. Crops Prod.* 79, 170-179.



- 460** Liu, W-J., Tian, K., Jiang, H., Yu, H-Q., 2013. Facile synthesis of highly efficient and  
**461** recyclable magnetic solid acid from biomass waste. *Sci. Rep.* 3, 2419.
- 462** Lou, H., Yuan, L., Qiu, X., Qiu, K., Fu, J., Pang, Y., Huang, J., 2016. Enhancing enzymatic  
**463** hydrolysis of xylan by adding sodium lignosulfonate and long-chain fatty alcohols. *Bioresour.*  
**464** *Technol.* 200, 48–54.
- 465** Moreira, L. R. S., Filho, E. X. F., 2016. Insights into the mechanism of enzymatic hydrolysis of  
**466** xylan. *Appl. Microbiol. Biotechnol.* 100, 5205-5214.
- 467** Nakasu, P. Y. S., Ienczak, L. J., Costa, A. C., Rabelo, S.C., 2016. Acid post-hydrolysis of  
**468** xylooligosaccharides from hydrothermal pretreatment for pentose ethanol production. *Fuel.* 185,  
**469** 73-84.
- 470** Negahdar, L., Delidovich, I., Palkovits, R., 2016. Aqueous-phase hydrolysis of cellulose and  
**471** hemicelluloses over molecular acidic catalysts: Insights into the kinetics and reaction  
**472** mechanism. *Appl. Catal., B.* 184, 285-298.
- 473** Oh, Y. H., Eom, I. Y., Joo, J. C., Yu, J. H., Song, B. K., Lee, S. H., Hong, S. H., Park, S. J.,  
**474** 2015. Recent advances in development of biomass pretreatment technologies used in  
**475** biorefinery for the production of bio-based fuels, chemicals and polymers. *Korean J. Chem.*  
**476** *Eng.* 32, 1945.
- 477** Ormsby, R., Kastner, J. R., Miller, J., 2012. Hemicellulose hydrolysis using solid acid catalysts  
**478** generated from biochar. *Catal. Today.* 190, 89- 97.
- 479** Prückler, M., Siebenhandl-Ehn, S., Apprich, S., Höltinger, S., Haas, C., Schmid, E., Kneifel,  
**480** W., 2014. Wheat bran-based biorefinery 1: Composition of wheat bran and strategies of  
**481** functionalization. *LWT Food Sci. Technol.* 56, 211-221.
- 482** Putro, J. N., Soetaredjo, F. E., Lin, S-Y., Ju, Y-H., Ismadji, S., 2016. Pretreatment and  
**483** conversion of lignocellulose biomass into valuable chemicals. *RSC Adv.* 6, 46834-46852.

- 484** Romero, A., Alonso, E., Sastre, Á., Nieto-Márquez, A., 2016. Conversion of biomass into  
**485** sorbitol: cellulose hydrolysis on MCM-48 and D-glucose hydrogenation on Ru/MCM-48.  
**486** Microporous Mesoporous Mater. 224, 1-8.
- 487** Sahu, R., Dhepe, P.L., 2012. A one-pot method for the selective conversion of hemicellulose  
**488** from crop waste into C5 sugars and furfural by using solid acid catalysts. ChemSusChem. 5,  
**489** 751-761.
- 490** Salmi, T., Murzin, D., Wärna, J., Mäki-Arvela, P., Kusema, B., Holmbom, B., Willför, S., 2014.  
**491** Hemicellulose hydrolysis in the presence of heterogeneous catalysts. Topics in Catalysis. 57,  
**492** 1470-1475.
- 493** Sánchez-Bastardo, N., Romero, A., Alonso, E., 2017. Extraction of arabinoxylans from wheat  
**494** bran using hydrothermal processes assisted by heterogeneous catalysts. Carbohydr. Polym. 160,  
**495** 143-152.
- 496** Shimizu, K-I., Furukawa, H., Kobayashi, N., Itaya, Y., Satsuma, A., 2009. Effects of Brønsted  
**497** and Lewis acidities on activity and selectivity of heteropolyacid-based catalysts for hydrolysis  
**498** of cellobiose and cellulose. Green Chem. 11, 1627-1632.
- 499** Singhvi, M. S., Chaudhari, S., Gokhale, D. V., 2014. Lignocellulose processing: a current  
**500** challenge. RSC Adv. 4, 8271.
- 501** Sluiter, A., Hames, B., Ruiz, R., Scarlata, C., Sluiter, J., Templeton, D., 2008. Determination of  
**502** Sugars, Byproducts, and Degradation Products in Liquid Fraction Process Samples. Laboratory  
**503** Analytical Procedure (LAP). Technical Report NREL/TP-510-42623.
- 504** Tathod, A., Kane, T., Sanil, E. S., Dhepe, P. L., 2014. Solid base supported metal catalysts for  
**505** the oxidation and hydrogenation of sugars. J. Mol. Catal. A: Chem. 388-389, 90-99.
- 506** Vilcocq, L., Castilho, P. C., Carvalheiro, F., Duarte, L. C., 2014. Hydrolysis of oligosaccharides  
**507** over solid acid catalysts: A review. ChemSusChem. 7, 1010-1019.

- 508** Wang, J., Xu, W., Ren, J., Liu, X., Lu, G., Wang, Y., 2011. Efficient catalytic conversion of  
**509** fructose into hydroxymethylfurfural by a novel carbon-based solid acid. *Green Chem.* 13, 2678-  
**510** 2681.
- 511** Xue, P., Lu, G., Guo, Y., Wang, Y., Guo, Y., 2004. A novel support of MCM-48 molecular  
**512** sieve for immobilization of penicillin G acylase. *J. Mol. Catal. B: Enzym.* 30, 75-81.
- 513** Zhang, J., Zhuang, J., Lin, L., Liu, S., Zhang, Z., 2012. Conversion of D-xylose into furfural  
**514** with mesoporous molecular sieve MCM-41 as catalyst and butanol as the extraction phase.  
**515** *Biomass Bioenergy.* 39, 73-77.
- 516** Zheng, F-C., Chen, Q-W., Hu, L., Yan, N., Kong, X-K., 2014. Synthesis of sulfonic acid-  
**517** functionalized Fe<sub>3</sub>O<sub>4</sub>@C nanoparticles as magnetically recyclable solid acid catalysts for  
**518** acetalization reaction. *Dalton Trans.* 43, 1220-1227.
- 519** Zhou, L., Shi, M., Cai, Q., Wu, L., Hu, X., Yang, X., Chen, C., Xu, J., 2013. Hydrolysis of  
**520** hemicellulose catalyzed by hierarchical H-USY zeolites – The role of acidity and pore structure.  
**521** *Microporous Mesoporous Mater.* 169, 54-59.